Investigating, Forecasting and Proposing Emissions-Mitigation Pathways for CO_2 Emissions from Fuel Combustion Only for the United States and Canada

by

*__Bismark Ameyaw__, School of Management and Economics, University of Electronic Science and Technology of China; Center for West African Studies, University of Electronic Science and Technology of China; No.2006, Xiyuan Ave, West Hi-Tech Zone, 611731, Chengdu, Sichuan, P.R. China., +8613693498270; 201714110101@std.uestc.edu.cn

Professor Li Yao, School of Management and Economics, University of Electronic Science and Technology of China, No. 2006, Xiyuan Ave, West Hi-Tech Zone, Chengdu 611731, Sichuan, China, +8613551008140, liyao@uestc.edu.cn; East Asian Institute, National University of Singapore, No. 469 Bukit Timah Road, 259756, Singapore

Amos Oppong, School of School of Management and Economics, University of Electronic Science and Technology of China; Center for West African Studies, University of Electronic Science and Technology of China; No.2006, Xiyuan Ave, West Hi-Tech Zone, 611731, Chengdu, Sichuan, P.R. China., +8615608219396; oppong.amos@gmail.com

Kingsley Nketia Acheampong, School of Information and Software Engineering, University of Electronic Science and Technology of China; No.2006, Xiyuan Ave, West Hi-Tech Zone, 611731, Chengdu, Sichuan, P.R. China, +8618602866370; nketiakingsley@gmail.com

ABSTRACT

In this study, we investigate the direction of causal relationship between carbon dioxide (CO_2) emissions from fossil fuel combustion only ($FFCO_2$) and economic growth for the US and Canada by using annual time series data for the period 1990-2016. We found a unidirectional causality running from gross domestic product per capita to $FFCO_2$ in the case of the US and Canada, and a unidirectional causality running from total labor force to $FFCO_2$ for the US and Canada. Second, with the quest to achieve cleaner energy targets, we formulate a mathematically induced algorithm based on an Artificial Neural Network (ANN) approach to forecast $FFCO_2$ for the US and Canada. Finally, we propose emission-mitigation pathways for these countries to follow to achieve zero $FFCO_2$ by the year 2030. Results from the optimal mitigation path demonstrate that intensifying current and introducing new policies are enough to mitigate energy-related $FFCO_2$ for all the countries employed herein.

Keywords: CO_2 emissions from combustion; Artificial Neural Network (ANN); Climate Change; Forecast evaluation.

1. Introduction

For growing importance of energy-related emissions, climate scientist have indicated that there have been rapid increase in carbon dioxide (CO_2) concentrations in the atmosphere (with significant increase in the levels of methane (CH4) and nitrous oxide (N2O)) as compared to the pre-industrial era level of about 280 parts per million (ppm) (International Energy Agency-U.S., 2016). Over the past century, human activities related to production and consumption are responsible for the increase in greenhouse gas (GHG) emissions in the atmosphere (Ameyaw and Yao, 2018). Considering human activities-led GHG emissions by source, carbon dioxide (CO_2) emissions from fossil fuel combustion only ($FFCO_2$) is a significant contributor to total GHG gas emissions (Rutherford, 2017). Against this backdrop, emissions from $FFCO_2$ should be of utmost concern due to their growing magnitude, the concomitant adjustments in climate and its direct impact on ecosystems and energy demand (Andres, 2012). These human-led adjustments in the ecosystem and climate change could hurt human society (Gambo et al., 2018). Such alterations in the ecosystem and climate change has caused many economies to develop a low-carbon consuming economy to mitigate $FFCO_2$ (Menyah and Wolde-rufael, 2012).

In developing a low-carbon world, the year 2015 saw a milestone in climate action with the negotiation at the 21st Conference of the Parties (COP21) of the Paris Agreement which extends mitigation obligations to all parties involved (Zhang et al., 2017). The Agreement notably hinges on the collective approach to sustain the increase in global average temperature to well below two-degrees-Celsius (2°C) above pre-industrial levels and to develop strategies to limit temperature increase to 1.5°C (ICF International, 2016). To achieve these set objectives, parties aim to reach peaking of GHG emissions globally to achieve a balance between anthropogenic emissions by sources and removals by sinks of GHGs in the second half of this century. For the Agreement's international action beyond the year 2020, a single framework is set to be developed to track the progress of the nationally-determined contributions (NDCs) for all countries with built-in flexibility for Parties' in different circumstances. All Parties will report regularly on emissions, progress towards NDCs, adaptation actions, and means of implementation. Although the Paris Agreements and previous Agreements like the Kyoto Protocol, Copenhagen Accord and Cancún Agreements aims at mitigating global GHG emissions, there has been an increasing concern as to sustainability and the validity of these agreements (Keohane and Victor, 2016). On a collaborative mitigation point of view, whether governments will ultimately agree to cooperate by investing in institutions depends on the preference because major countries vary in population, affluence, technology, and vulnerability to climate impacts that could alter emissions trajectories. Such diversity in the circumstances leads to considerable variations in the preferences of countries. Furthermore, agreement with the highest potential for collaborative gains most often cannot be structured in a self-enforcing manner thus creating a trade-off between greater potential benefits and an increased likelihood for achieving at least some collaboration. On an economic perspective, mitigating emissions proves to be complicated because of the energy demand that adds-in to economic development has to be taken into consideration.

Contributing to literature about the validity and sustainability of collaborative Agreements, accurate evaluation and adjustments of energy policies, as well as fast and reasonable estimates of emissions mitigation pathways, is required as often as possible (Keohane and Victor, 2016). In addressing these loopholes in literature, as most research works focus on forecasting total CO_2 emissions, it is yet unclear how mitigating the amount of $FFCO_2$ can help in achieving the ultimate goal of sustainability. In filling this gap, we provide readers with the opportunity of knowing the impact of some macroeconomic variables on $FFCO_2$ as well as forecasting the amount of $FFCO_2$ and propose emissions-mitigation pathways for the USA and Canada to the year 2030. The empirical study analyzes the determinants between $FFCO_2$ which is lacking in the literature. We then formulate an artificial neural network (ANN) algorithm-a non-assumption driven univariate forecasting technique to forecast $FFCO_2$. Aside from the normal seasonality and trend modeled in an algorithm to improve the predictive accuracy of an algorithm, we introduce an element called 'holiday effect' in our algorithm formulation to enhance our predictive accuracy better. The holiday effect introduced in the algorithm formulation caters to discretized events with a high surety of occurrence. Such $FFCO_2$ scenarios are also lacking in the literature. Finally, with the quest to achieve cleaner energy targets, we propose $FFCO_2$ emissions mitigation pathways with the aim of achieving zero-emissions from $FFCO_2$ by the year 2030. Such emission mitigation pathways are also lacking in the literature. We use the United States and Canada as our case study. The United States (US) is employed herein because it is the second largest emitter of CO_2 (Steeves and Ouriques, 2016). Also, the US is speculated to have withdrawn from the Paris Agreement which aims for global emissions mitigation (Rutherford, 2017). Canada is also employed as a case study because it is asserted that Canada is likely to miss its Paris Agreement NDC to mitigate industrial wide GHG emissions by 30 percent (%) below 2005 levels by 2030 ("Canada's Climate Action Tracker," 2017).

2. Model and Data

2.1 Econometric Approach

Due to data uniformity, we use Gross Fixed Capital Formation (GFCF) which is measured as a percentage of Gross Domestic Product (% of GDP), Total labor force (LF) and Gross Domestic Product per capita (GDPC) as our main determining variables of $FFCO_2$ covering the period 1990-2016. The World Development Indicators (WDI) and the International Energy Agency (IEA) statistics portal are the data source. All variables except variables in ratio forms are transformed into natural logarithms to help mobilize stationarity in the variance-covariance matrix. We employ the Pesaran cross-sectional dependency test (Pesaran, 2004). We model the empirical method as:

$$FFCO_{2it} = \alpha_i + \beta_{it} x_{it} + \varepsilon_{it} \tag{1}$$

Where $i = 1, 2$ the subscript of the countries is used; $t = 1, 2, \ldots, T$ is the time dimension; β_{it} represents the coefficients of our determining variables; x_{it} represents each determining variable; α_i indicates the constant parameters and ε_{it} is our error term. We define both our null and alternative hypothesis as:

$$Null: x_{ij} = x_{ji} = cor(\varepsilon_{it}, \varepsilon_{jt}) = 0 \text{ for } i \neq j \tag{2}$$

$$Alternative: x_{ij} = x_{ji} \neq 0 \text{ for } i \neq j \tag{3}$$

Mathematically, $x_{ij} = x_{ji}$ becomes:

$$\frac{\sum_{t=1}^{T} \varepsilon_{it} \varepsilon_{jt}}{\left(\sum_{t=1}^{T} \varepsilon^2{}_{it}\right)^{\frac{1}{2}} \left(\sum_{t=1}^{T} \varepsilon^2{}_{jt}\right)^{\frac{1}{2}}} \tag{4}$$

For our test sample, we employ (Pesaran, 2004) which serves as an improvement on (Breusch and Pagan, 1980) Lagrange multiplier test (LM). Pesaran's version of the LM test is calculated as:

$$\sqrt{\frac{2T}{N(N-1)}} \sum_{i=1}^{N-1} \sum_{j=i+1}^{N} \tau_{ij} \rightarrow N(0,1) \tag{5}$$

Where τ_{ij} represents the residual coefficients of our panel model.

After the cross-sectional dependency test, we check for heterogeneous autoregressive coefficients by employing the Im, Pesaran, and Shin (IPS) (Im et al., 2003). We develop the heterogeneous autoregressive coefficients mathematically as:

$$\Delta FFCO_{2it} = x_i FFCO_{2it-1} + \delta_i X_{it} + \varphi_{it} \tag{6}$$

Where X_{it} represents our determining variables comprising specific time trend; x_i is the autoregressive coefficients, and φ_{it} represent the stationary residuals. In eliminating evidence of any autocorrelation in (6), we turn to the exploration of high order differential delay terms formulated by (Levin et al., 2002) as:

$$\Delta FFCO_{2it} = x_i FFCO_{2it-1} + \sum_{j=1}^{x_i} \phi_{ij} \Delta FFCO_{2it-1} + \delta_i X_{it} + \varphi_{it} \tag{7}$$

Where the number of lags is represented by x_i. With the Augmented Dickey-Fuller (ADF) test, we develop the null hypothesis as there exists unit root in each series of our datasets whereas the alternative hypothesis is the case where at least one individual series is stationary.

After the confirmation of a stationarity pattern in our sequence, co-integration test developed by (Pedroni, 2004) is used. We develop the heterogeneous co-integration equation as:

$$FFCO_{2it} = \alpha_i + \delta_{it} + \beta_{1i} X_{1i,t} + \beta_{2i} X_{2i,t} + \beta_{3i} X_{3i,t} + \beta_{4i,t} X_{4i,t} + \varphi_{it} \tag{8}$$

Where α_i and δ_i represents each country's deterministic trends; φ_{it} represents the residuals as a result of deviations from the long-run relationships. We propose our null and alternative hypothesis as there is no and there is co-integration between our variables in the long-run.

After the co-integration analysis, we utilize the Granger causality test (Granger, 1969) to analyze the influence of one data sequence on another. We define our null hypothesis as a particular data sequence does not Granger-cause another data sequence. Mathematically, we formulate the Granger causality test as:

$$FFCO_{2t} = \alpha_0 + \sum_{i=1}^{r} \alpha_i FFCO_{2t-i} + \sum_{i=1}^{r} \beta_i x_{t-i} + \varphi_t \tag{9}$$

$$x_t = \alpha_0 + \sum_{j=1}^{r} \alpha_j FFCO_{2t-j} + \sum_{j=1}^{r} \beta_j x_{t-j} + \varphi_t \tag{10}$$

2.2 ANN Automated Structural forecasting Approach

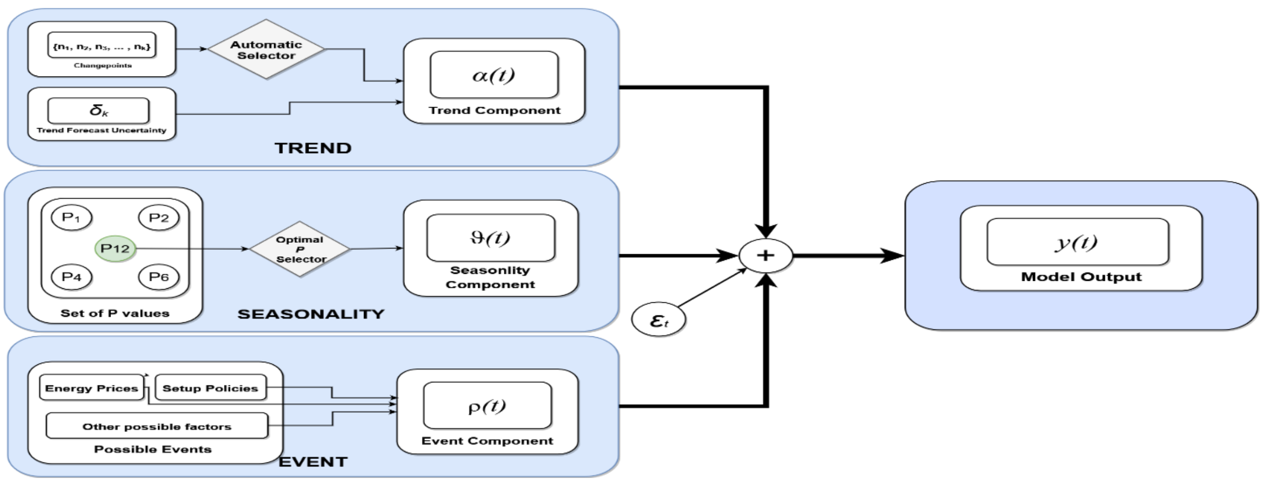

Figure 1: Summary of Authors methods on the application of the ANN technique

Most machine learning models are deduced on the component of trends and seasonality but sometimes fail to capture discretized effects that may cause a shift in a dataset (Suganthi and Samuel, 2012). Here, we follow a decomposable time series model leveraging trend, seasonality, and 'holiday effects' as its components. We denote its structural modules as:

$$y(t) = \alpha(t) + \vartheta(t) + \rho(t) + \varepsilon_t \tag{11}$$

Where $\alpha(t)$ and $\vartheta(t)$ represent the trend and seasonality component respectively. $\rho(t)$ is the consumption variations (holiday effects) that occur on an irregular schedule or time (t). ε_t represents any subtle changes that our model does not accommodate.

2.2.1 Non-linear trend with changepoints

YoY patterns of energy consumption could portray varying rates of growth. Therefore, we formulate our trend component to cater for the different growth to uniquely mimic non-linear saturating growths. To improve the predictive accuracy of our algorithm, a carrying capacity similar to a logistic function different from other non-linear saturating growths is formulated. The carrying capacity is represented mathematically as:

$$\alpha(t) = \frac{C}{1+e^{-g\left(t-p_{off}\right)}} \tag{12}$$

Where *C* – carrying capacity, *g* – growth rate, p_{off} - an offset parameter

Meanwhile, the carrying capacity of the $FFCO_2$ may not be constant, and the growth rate might not be constant either. Therefore, instead of a carrying capacity $FFCO_2$, we use as a time-varying capacity $C\left(t\right)$. The time-varying capacity $C\left(t\right)$ as presented in the model is a parameter set that contains the anticipated capacities of the system at any time $\left(t\right)$. Several econometric factors may cause a shift in $FFCO_2$. These factors make us add a different growth rate to fit the datasets. We make changepoints definitions in the trend model where the growth rate is permitted to change by using 'rate adjustments' vector, $\delta \in R^N$ assuming there exist N changepoints at n_k times; where $k=1,...,N$ and δ_k is the change in rates that occurs at a time n_k. The rate at any time t is, therefore, the sum of the base rate *g*, and all the adjustment to that point, that is,

$$g + \sum_{k:t>n_k} \delta_k \tag{13}$$

Defining a vector *v as*

$$v(t) \in \{0,1\}^N \text{ Where } v_k(t) = \begin{cases} 1, & \text{if } t \geq n_k, \\ 0, & otherwise \end{cases}, \tag{14}$$

Then the rate at a time t becomes $g + v(t)^{\mathrm{T}}\delta$. With this established, the adjustment, γ at changepoints k, when the p_{off} is successfully connected to the ending points of the segment would be:

$$\gamma_k = (n_k - p_{off} - \sum_{l<k}\gamma l)(1 - \frac{g+\sum_{l<k}\delta_l}{g+\sum_{l<k}\delta_l}) \tag{15}$$

And hence, the trend component of our forecast algorithm becomes a piecewise logistic growth model:

$$\alpha(t) = \frac{C(t)}{1 + e^{(-(g+v(t)^{\mathrm{T}}\delta)(t-(p_{off}+v(t)^{\mathrm{T}}\gamma)))}} \tag{16}$$

2.2.2 Trend Forecast Uncertainty

By extrapolation, we formulate our algorithm as such that takes care of individual trends in our datasets. As N changepoint over a history of T points, each of which has a rate change δ_k ~ Laplace (0*;* *τ*), we simulate future rate changes that mimic the past by substituting *τ* with an inferred variance from the data. The future changepoints are then sampled randomly so that the average frequency of changepoints corresponds to the past in (17).

$$\forall k > T, \begin{cases} \delta_k = 0 & \text{w.p. } \dfrac{T-N}{T}, \\ \delta_k \approx Laplace(0,\lambda) & \text{w.p. } \dfrac{S}{T}. \end{cases} \tag{17}$$

2.2.3 Seasonality

By using Fourier series with P as the regular period, we expect our datasets to have a seasonality index. We approximate arbitrary smooth seasonal effects with a standard Fourier series:

$$\mathrm{s(t)} = \sum_{n=1}^{N}\left(\left(a_n \cos\left(\frac{2\pi nt}{P}\right) + b_n \sin\left(\frac{2\pi nt}{P}\right)\right)\right) \tag{18}$$

After tuning our model, P of 12 months was our optimal P selector. Seasonality fitting requires estimating $2N$ parameters $\beta = [a_1, b_1, ..., a_N, \mathrm{b}_N]^T$. After the optimal selector, a matrix of seasonality vectors of each time t in our historical and future projections is constructed. The seasonality component becomes:

$$s(t) = X(t)\beta. \tag{19}$$

2.2.4 Holiday effects/Events

Events/holidays capture the predictable shocks in our datasets. Incorporating events/holidays in our algorithm formulation connotes assuming that the effects of holidays are independent of trend and seasonality. Therefore, for each event i, D_i represents the past and future dates for that event. We add an indicator function representing whether time t occurs at a particular holiday/event i and assign each event a parameter κ_i . This is done by generating a matrix of regressors:

$$Z(t) = \left[1(t \in D_1), \ldots, 1(t \in D_L)\right] \tag{20}$$

2.3 Mitigation Technique for FFCO₂

For post-2016 $FFCO_2$ projections, data covering the period of 1990-2010 inclusive are used as our training datasets. Emissions projections from 2011-2016 inclusive are used as our benchmark test set to make forecasting projections and mitigation pathways from 2017-2030 inclusive. In estimating our emission-mitigation pathways, we established an emission target of negative, zero or one for $FFCO_2$. We then set an optimal mitigation path as one that registers a high predictive accuracy of at least ninety-eight percent (98%) for our test sets with future emission levels that mimic the decreasing trends by approaching zero or negative.

2.4 Error Indexes

Here, we measure errors from our BiLSTM model output using the YoY errors, mean absolute deviation (MAD), mean absolute percentage error (MAPE) and root mean square error (RMSE) (Ameyaw and Yao, 2018). Denoting our observed values in a particular year as O_t and F_t as our forecasted values for a specific year, the YoY errors is formulated as:

$$\lambda_t = \frac{|O_t - F_t|}{O_t} \tag{21}$$

Where O_t and F_t are the observed and forecast values for $FFCO_2$ respectively. Results (21) are deemed an undercast if $R_t > F_t$ or of an overcast if $F_t > R_t$. We calculate the MAD, MAPE, and RMSE error indexes as:

$$MAD = \frac{\sum_{t=1}^{n} \lambda_t}{n} \tag{22}$$

$$MAPE = \left[\frac{100}{n}\left(\sum_{t=1}^{n} \frac{\lambda_t}{O_t}\right)\right] \tag{23}$$

$$RMSE = \sqrt{\frac{\sum_{t=1}^{n} (\lambda_t)^2}{n}} \tag{24}$$

Where *n* is the number of the period in years.

Although we use MAD and RMSE in evaluating the predictive accuracy of our formulated algorithm, MAPE is used as our main benchmark error index because there are no extreme values in our data sets including zeros.

3. Empirical Data Analysis

3.1 Econometric Approach

3.1.1 Cross-Sectional Dependence Analysis

The results of the Pesaran cross-sectional dependence test is shown in Table 1. As it is evident from Table 1 that the *p*-value is below 5%, we conclude that cross-sectional dependency should be utilized before stationarity and co-integration relationships are analyzed.

Table 1. Cross-sectional dependence test.

Cross-Sectional Dependence Test	Pesaran's Test	*p*-Value
	US	
Pesaran's Test	3.6849	0.0253 [y]
	CANADA	
Pesaran's Test	3.5827	0.0197[y]

Footnote: [y] represents a 5% significance level.

3.1.2. Stationarity Analysis

For the stationarity analysis, we use the Levin, Lin, and Chu (L.L&C), Augmented Dickey-Fuller, IPS, and Phillips–Perron Fisher (PP-Fisher) tests. The results of our panel unit root examination are presented in Table 2. From Table 2, we conclude that variables are not stationary at level but stable at first differencing.

Table 2. Panel unit root results.

Form	Variables	L.L&C	IPS	ADF	PP-Fisher	Conclusions
			US			
Level	$lnFFCO_2$	0.7532 (0.7368)	0.3564 (0.5983)	0.7191 (0.6037)	1.3899 (0.3784)	Non-stationary
	GDPC	0.6891 (0.6582)	1.9332 (0.9173)	0.5728 (0.9428)	0.0482 (0.9682)	Non-stationary
	lnLF	−1.2382 (0.2920)	−0.3873 (0.3649)	1.8320 (0.3289)	1.4897 (0.4928)	Non-stationary
	GFCF	−0.5803 (0.1893)	0.2894 (0.3702)	1.8739 (0.3492)	1.0478 (0.6397)	Non-stationary
First Difference	Δ $lnFFCO_2$	−1.2513 (0.0392) [y]	−0.9527 (0.0402) [y]	4.6891 (0.0447) [y]	6.8024 (0.0469) [y]	Stationary
	Δ GDPC	−2.5856 (0.0005) [x]	−1.9274 (0.0264) [y]	6.9357 (0.0317) [y]	10.6134 (0.0021) [x]	Stationary
	Δ lnLF	−1.8397 (0.0001) [x]	−1.3492 (0.0017) [x]	7.9582 (0.0021) [x]	9.5983 (0.0004) [x]	Stationary
	Δ GFCF	−0.4294 (0.0203) [y]	−0.1793 (0.0217) [y]	5.8937 (0.0289) [y]	7.6743 (0.0185) [y]	Stationary
			CANADA			
Level	$lnFFCO_2$	0.6214 (0.2368)	0.4567 (0.3878)	0.5161 (0.2337)	1.4899 (0.2981)	Non-stationary
	GDPC	0.2687 (0.3658)	2.1859 (0.4790)	0.4567 (0.2643)	0.2741 (0.5697)	Non-stationary
	lnLF	−2.1782 (0.3140)	−0.4692 (0.3111)	1.9720 (0.2789)	1.8767 (0.4508)	Non-stationary
	GFCF	−0.4603 (0.2753)	0.3902 (0.3759)	1.9794 (0.2894)	1.3958 (0.5697)	Non-stationary

First Difference	Δ $lnFFCO_2$	−1.3217 (0.0291) ^{y}	−0.8427 (0.0102) ^{y}	3.7891 (0.0217) ^{y}	6.5899 (0.0369) ^{y}	Stationary
	Δ GDPC	−2.3456 (0.0001) ^{x}	−1.7492 (0.0344) ^{y}	6.5794 (0.0417) ^{y}	10.8321 (0.0001) ^{x}	Stationary
	Δ lnLF	−1.7491 (0.0001) ^{x}	−1.2386 (0.0001) ^{x}	7.1456 (0.0002) ^{x}	9.8349 (0.0001) ^{x}	Stationary
	Δ GFCF	−0.2994 (0.0210) ^{y}	−0.2197 (0.0189) ^{y}	5.9217 (0.0307) ^{y}	7.658 (0.0281) ^{y}	Stationary

Notes: Values in brackets represents the probabilities. ^{x} represents a 1% significance level, and ^{y} represents a 5% significance level.

3.1.3. Co-Integration Test

After establishing that all our variables employed herein are stationary at first differencing, we perform Pedroni co-integration analysis to check the long-run relationship between our variable data sequences in Table 3. The result of our co-integration test reveals that there exist long-run relationship amongst our variables of the study.

Table 3. Co-integration test result.

US			
Method	**Test Statistics**	**Value**	**Probability**
Pedroni	Panel v-Statistics	−1.3284	0.0194 ^{y}
	Panel rho-Statistics	−1.2190	0.0279 ^{y}
	Panel PP-Statistics	−5.1194	0.0051 ^{x}
	Panel ADF-Statistics	−1.6436	0.0004 ^{x}
	Group rho-Statistics	−1.5973	0.0217 ^{y}
	Group PP-Statistics	−7.3932	0.0010 ^{x}
	Group ADF-Statistics	−1.4828	0.0018 ^{x}
CANADA			
Method	**Test Statistics**	**Value**	**Probability**
Pedroni	Panel v-Statistics	−1.9087	0.0231 ^{y}
	Panel rho-Statistics	−1.3124	0.0189 ^{y}
	Panel PP-Statistics	−4.6532	0.0043 ^{x}
	Panel ADF-Statistics	−1.4678	0.0000 ^{x}
	Group rho-Statistics	−1.0086	0.0171 ^{y}
	Group PP-Statistics	−6.1129	0.0000 ^{x}
	Group ADF-Statistics	−1.4633	0.0000 ^{x}

Notes: ^{x} indicates a 1% level of confidence and ^{y} suggests a 5% level of confidence.

3.1.4. Granger Causality Analysis

Table 4 depicts the results of the Granger causality analysis. Here, we establish that if the probability values in brackets are less than 5% significance level, then there is evidence of a Granger causality relationship. From our analysis, we conclude that there exists a unidirectional causal relationship running from GDPC to $FFCO_2$ emissions and from LF to $FFCO_2$ emissions. However, there exists no causal relationship between GFCF and $FFCO_2$ emissions for both the US and Canada.

Table 5. Results for Granger causality test.

Null Hypothesis	US	CANADA
GDPC does not Granger cause $lnFFCO_2$	12.3142 (0.0011) ^{x}	8.9852 (0.0004) ^{x}
$lnFFCO_2$ does not Granger cause GDPC	1.1274 (0.1585)	1.1946 (0.2742)
lnLF does not Granger cause $lnFFCO_2$	9.7839 (0.0382) ^{y}	11.2674 (0.0288) ^{y}
$lnFFCO_2$ does not Granger cause lnLF	2.6542 (0.1178)	2.9459 (0.1830)
GFCF does not Granger cause $lnFFCO_2$	4.5921 (0.6821)	5.4298 (0.8468)
$lnFFCO_2$ does not Granger cause GFCF	1.5967 (0.3247)	1.9678 (0.3957)

Notes: the values in brackets indicates the probability values. ^{x} indicates 1% level of confidence and ^{y} indicates 5% level of confidence.

3.2 ANN Approach

3.2.1 Testing Stage

Here data obtained from IEA for total $FFCO_2$ in metric tons of CO_2 is employed. Checking for the predictive accuracy of the ANN approach, ANN projections covering the period of 2011-2016 inclusive for the US and Canada are presented in Figure 2. From Figure 2, the ANN approach testing stage output performed well against the observed values for the US and Canada (see Figure 2a and 2b). ANN test output YoY errors for US is ~0.25%, ~0.51%, ~0.90%, ~0.13%, ~0.41%, and ~0.29% for the period covering 2011-2016 (inclusive) respectively. MAD of ~60.55 and RMSE of ~80.27 with MAPE accuracy of 98.78% achieved. Canada's YoY errors are ~1.28% for 2011, ~2.33% for 2012, ~0.99% for 2013, ~2.32% for 2014, ~2.31% for 2015, and ~1.02% for 2016. We record the MAPE accuracy of ~98.21% with a MAD and RMSE value of ~9.25 and ~9.84 respectively.

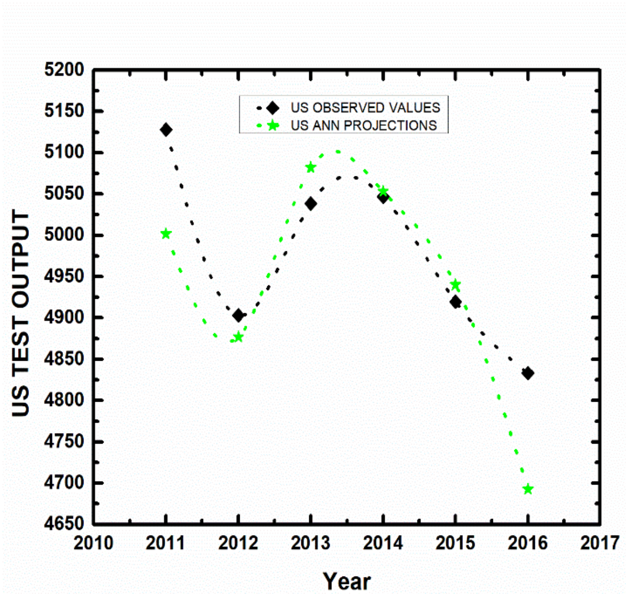

(a)

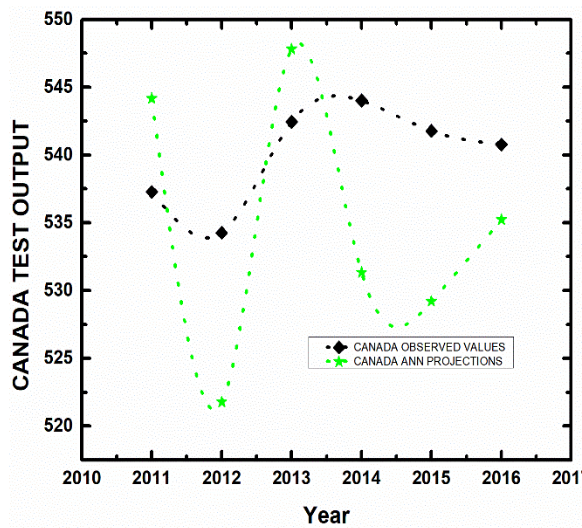

(b)

Figure 2: ANN test output performance against observed values for the period covering 2011–2016.

3.3 $FFCO_2$ Forecasting and Mitigation Pathways

3.3.1 $FFCO_2$ Forecasting

Based on the testing stage performance of our ANN approach, we forecast $FFCO_2$ from 2017-2030 inclusive for all the countries employed herein. For USA, emissions will hit ~3187.43MtCO_2 in 2020, ~2021.89MtCO_2 in 2025, and ~977.46MtCO_2 in 2030 (see Figure 3a). Canada's emissions will be ~489.23MtCO_2 in 2020, ~421.36MtCO_2 in 2025, and ~319.34MtCO_2 in 2030 (see Figure 3b).

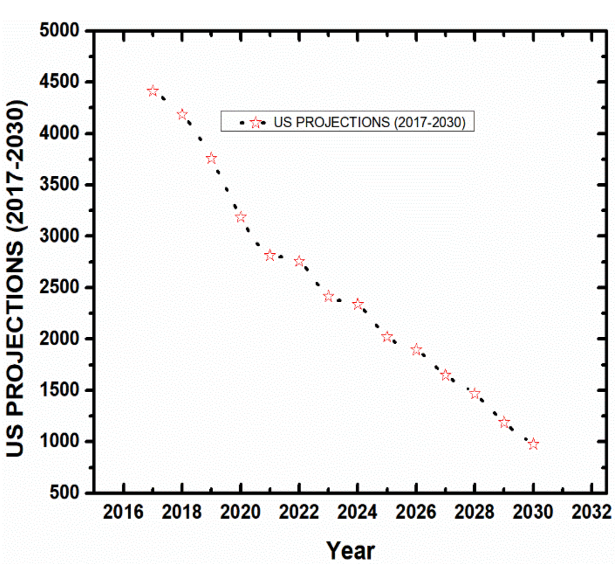

(a)

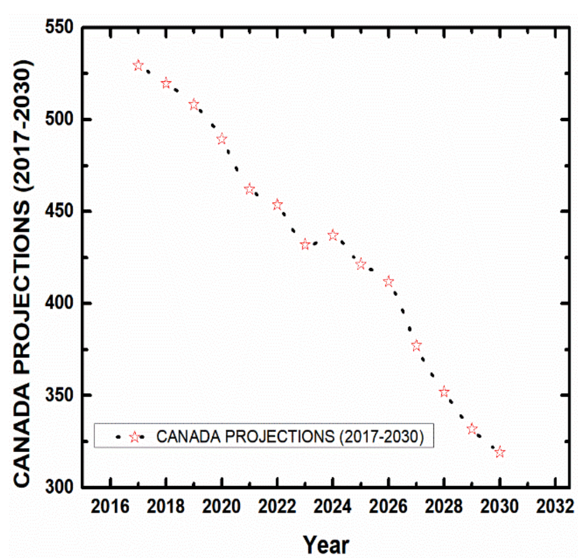

(b)

Figure 3: ANN forecast projections for $FFCO_2$

3.3.2 $FFCO_2$ Mitigation Pathways

For our emission mitigation pathways propose in Figure 4a and 4b, emissions projections for the period covering 2011-2016 is used as a test set although National Energy Modelling Systems (NEMS) has recommended that a test set of three-years is justifiable for emission mitigation pathways. To ensure the predictive accuracy and performance of our mitigation pathways, we decided to look back for seven years. $FFCO_2$ data obtained from IEA depicts a decreasing trend. Thus, the decreasing patterns in data coupled with the prerogative of switching to the use of renewables make it imperative to state that emissions from $FFCO_2$ are expected to decline in the post-2016 period. Therefore, using our ANN algorithm formulation, we set a lower bound of zero emissions for the year 2030. To achieve zero $FFCO_2$ by 2030, the USA has to decrease $FFCO_2$ emissions from the current 2016 level of ~4833.08MtCO_2 to ~3391.41MtCO_2 and ~1716.18MtCO_2 by 2020 and 2025 respectively (see Figure 4a). Canada will have to decrease its 2016 emission level of ~540.77MtCO_2 to ~391.13MtCO_2 and ~205.63MtCO_2 by 2020 and 2025 respectively (see Figure 4b).

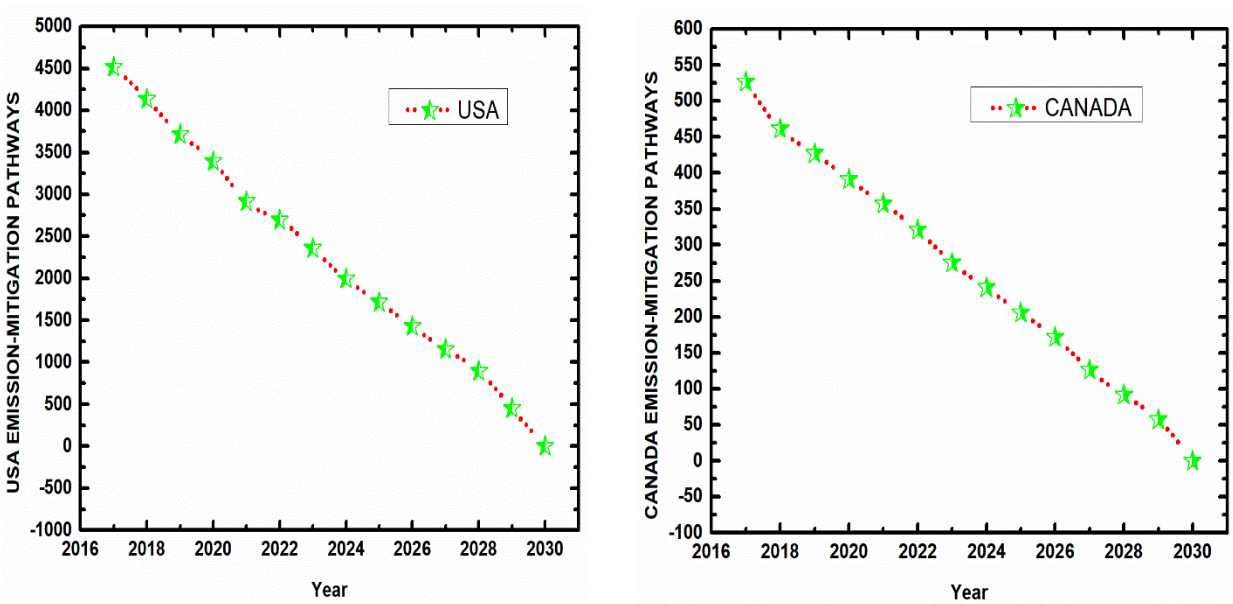

(a) (b)

Figure 4: Emission-mitigation pathways for $FFCO_2$

4. Conclusions and Recommendations

This paper first investigated the relationship between total $FFCO_2$ emissions, GDPC, LF, and GFCF in the US and Canada. The main conclusions drawn from our analysis for both the US and Canada is the existence of unidirectional causality running from GDPC to $FFCO_2$ emissions and from LF to $FFCO_2$ emissions. However, no evidence of causality was found between $FFCO_2$ emissions and GFCF for the countries employed herein. Therefore, concerning the results obtained, the US and Canada should diversify into alternative energy sources with lower greenhouse gas emissions. This will assist in reducing $FFCO_2$ emissions and at the same sustain long-run economic growth.

Second, after analyzing the nexus between $FFCO_2$, gross domestic product per capita, gross fixed capita formation, and labor force, we formulate our algorithm based on mathematically induced ANN approach to forecast (see Figure 3) and propose emission-mitigation pathways (see Figure 4) for $FFCO_2$ for the US and Canada. Our ANN approach algorithm formulation outperformed the 97% threshold set for forecasting (see Figure 2). We propose emission-mitigation pathways for the US and Canada to follow if they hope to achieve zero $FFCO_2$ by the year 2030 (see Figure 4). In order, to achieve zero $FFCO_2$ by the year 2030, the US and Canada should both intensify and implement mitigation measures such as the cap-and-trade system in ensuring an emission-free environment. Emission-mitigation measures should aim at promoting low carbon usage, penetrating and investing into the renewable energy sector, instituting a suitable and functional framework for climate change governance, scale up the adoption of efficient energy-saving technologies, and improving forest and solid waste management.

References

Ameyaw, B., Yao, L., 2018. Analyzing the impact of GDP on CO2 emissions and forecasting Africa's total CO2 emissions with non-assumption driven bidirectional long short-term memory. Sustain. 10. https://doi.org/10.3390/su10093110

Andres, R.J. et. al, 2012. Biogeosciences A synthesis of carbon dioxide emissions from fossil-fuel combustion. Biogeosciences 2, 1845–1871. https://doi.org/10.5194/bg-9-1845-2012

Breusch, T.S., Pagan, A.R., 1980. The Lagrange Multiplier Test and its Applications to Model Specification in Econometrics. Rev. Econ. Stud. 47, 239. https://doi.org/10.2307/2297111

Canada's Climate Action Tracker, 2017.

Gambo, S., Ishak, S.B., Ismail, N.W., Idris, M.M., 2018. Energy Consumption , Environmental Emissions, and Economic Growth : An Empirical Analysis in Nigeria. J. Humanity. Soc. Sci. 23, 11–22. https://doi.org/10.9790/0837-2302021122

Granger, C.W.J., 1969. Investigating Causal Relations by Econometric Models and Cross-spectral Methods. Econometrica 37, 424. https://doi.org/10.2307/1912791

ICF International, 2016. Analysis of Intended Nationally Determined Contributions (INDCs). New Clim. Institute.

Im, K.S., Pesaran, M.H., Shin, Y., 2003. Testing for Seasonal Unit Roots in Heterogeneous Panels. J. Econom. 115, 53–74. https://doi.org/10.1016/j.econlet.2004.06.018

International Energy Agency-U.S., 2016. Key CO2 Emissions Trends. IEA-Statistics.

Keohane, R.O., Victor, D.G., 2016. Cooperation and discord in global climate policy. Nat. Clim. Chang. 6, 570–575. https://doi.org/10.1038/nclimate2937

Levin, A., Lin, C.F., Chu, C.S.J., 2002. Unit root tests in panel data: Asymptotic and finite-sample properties. J. Econom. 108, 1–24. https://doi.org/10.1016/S0304-4076(01)00098-7

Menyah, K., Wolde-rufael, Y., 2012. CO2 emissions , nuclear energy , renewable energy and economic growth in the US. Energy Policy 38, 2911–2915. https://doi.org/10.1016/j.enpol.2010.01.024

Pedroni, P., 2004. Panel Cointegration: Asymptotic And Finite Sample Properties Of Pooled Time Series Tests With An Application To The Econometric Press, Vol. No. 3, pp . Economic Theory 20, 597–625. https://doi.org/10.1017/S0266466604203073

Pesaran, M.H., 2004. General Diagnostic Tests for Cross Section Dependence in Panels CESifo Wor, 255–260.

Rutherford, T.F., 2017. US Withdrawal from the Paris Agreement: Economic Implications of Carbon-Tariff Conflicts. Harvard Proj. Clim. Agreements Discussion, 17–89.

Steeves, B.B., Ouriques, H.R., 2016. Energy Security: China and the United States and the Divergence in Renewable Energy. Context. Int. 38, 643–662. https://doi.org/10.1590/S0102-8529.2016380200006

Suganthi, L., Samuel, A.A., 2012. Energy models for demand forecasting - A review. Renew. Sustain. Energy Rev. https://doi.org/10.1016/j.rser.2011.08.014

Zhang, S., Liu, X., Bae, J., 2017. Does trade openness affect CO2emissions: evidence from ten newly industrialized countries? Environ. Sci. Pollut. Res. 24, 17616–17625. https://doi.org/10.1007/s11356-017-9392-8